

Nonparametric Inference for Balance in Signed Networks

Xuyang Chen^{*†} Yinjie Wang^{*‡} Weijing Tang[§]

Abstract

In many real-world networks, relationships often go beyond simple dyadic presence or absence; they can be positive, like friendship, alliance, and mutualism, or negative, characterized by enmity, disputes, and competition. To understand the formation mechanism of such *signed networks*, the social *balance theory* sheds light on the dynamics of positive and negative connections. In particular, it characterizes the proverbs, “a friend of my friend is my friend” and “an enemy of my enemy is my friend”. In this work, we propose a nonparametric inference approach for assessing empirical evidence for the balance theory in real-world signed networks. We first characterize the generating process of signed networks with node exchangeability and propose a nonparametric sparse signed graphon model. Under this model, we construct confidence intervals for the population parameters associated with balance theory and establish their theoretical validity. Our inference procedure is as computationally efficient as a simple normal approximation but offers higher-order accuracy. By applying our method, we find strong real-world evidence for balance theory in signed networks across various domains, extending its applicability beyond social psychology.

1 Introduction

In many real-world complex systems, the relationships among subjects often extend beyond simple presence or absence. Apart from positive connections like friendship, alliance, and mutualism, relationships between two entities can also be negative, characterized by enmity, dispute, and competition. These multifaceted relationships among a group of subjects

*Xuyang Chen and Yinjie Wang are co-first authors and have made equal contributions.

†Department of Applied Mathematics and Computational Science, University of Pennsylvania.

‡Department of Statistics, University of Chicago.

§Department of Statistics and Data Science, Carnegie Mellon University.

can be represented as *signed networks*. A signed network consists of two elements, nodes, which are the basic units of the system, and edges, representing the positive or negative connections between the nodes. Such signed networks are ubiquitous in diverse engineering and scientific disciplines, such as biology, computer science, economics, and sociology, among others. Examples include social networks where friendships and animosities coexist [Leskovec et al., 2010], ecological networks depicting symbiotic and predatory relationships among species [Saiz et al., 2017], international relation networks indicating alliance and militarized disputes among countries [Kirkley et al., 2019], and protein-protein interaction networks describing both positive and negative associations [Huttlin et al., 2021].

Such signed networks have substantially different properties and principles from unsigned ones. One fundamental theory that elucidates the connectivity in signed networks is the *balance theory* [Heider, 1946, Cartwright and Harary, 1956]. Originated from social psychology, the balance theory posits that individuals strive for psychological consistency in their relationships and beliefs with others in their social environment. Specifically, balance theory focuses on triangular configurations where three individuals are connected to each other. These triangles, due to the nature of the signed relationships, can be categorized into four types (see Figure 1). A triangle achieves a balanced state when it contains an even number of negative edges. Balanced triangles align with common proverbs, “a friend of my friend is my friend” and “an enemy of my enemy is my friend”, corresponding to type-1 and type-3 triangles respectively. In contrast, an unbalanced state arises when relationships deviate from this pattern, leading to psychological discomfort. For example, in a type-2 triangle, where an individual has two friends who hold negative sentiments towards each other, the individual may reconcile two friends to restore balance.

Balance theory posits that triangles in a signed network tend to be balanced, which provides valuable insights into the dynamics of positive and negative connections. Existing work has demonstrated that properly leveraging the balance theory in modeling signed networks can improve goodness of fit, interpretability, and node and link prediction [Derr et al., 2018, Tang and Zhu, 2024, Hsieh et al., 2012, Chiang et al., 2014, Zhang and Wang, 2022]. However, balance theory is not universally applicable to all signed networks and improper application may lead to misleading results. Therefore, a crucial first step is to assess the empirical evidence for balance theory in real-world signed networks to investigate its applicability.

To this end, it requires appropriate extensions of the concept of balance from individual triangles to the entire signed network to measure the overall degree of balance. Harary [1953] introduced structural balance theory, where a signed network is balanced if all its triangles are balanced. Davis [1967] proposed a weaker version, saying that a signed network is weakly balanced if no type-2 triangles occur, *i.e.*, only triangles with two positive

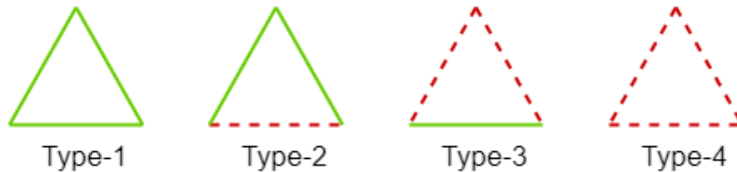


Figure 1: Four types of different triangles, where the green solid line represents a positive edge and the red dashed line represents a negative edge. Type-1 and type-3 triangles are balanced, type-4 triangle is weakly balanced, and type-2 triangle is unbalanced.

edges are impermissible and “the enemy of my enemy can be my enemy”. However, both structural and weak balance, which require all triangles to follow certain patterns, may be overly stringent for practical applications, especially for large signed networks. A natural quantity of interest is the count of balanced or weakly balanced triangles in an observed signed network. To account for noise in the observed networks, several studies have investigated the asymptotic properties of the normalized count under different balance-free models (*i.e.*, where the generated network is absent of balance) [Facchetti et al., 2011, Leskovec et al., 2010, Feng et al., 2022, Jin et al., 2024b]. Yet, beyond balance-free models, when the balance pattern is present, uncertainty quantification of normalized counts remains unclear.

In this work, we introduce a nonparametric inference method to measure the degree of balance in observed signed networks. The inference procedure constructs confidence intervals for the expected proportion of balanced (or weakly balanced) triangles. Notably, the validity of our inference method holds under various degrees of balance, including balance-free scenarios. Thus, in contrast to existing works, our inference approach provides insights into not only whether or not a network is balance-free but also *how balanced (or weakly balanced) a signed network is*. Specifically, we consider a broad range of node-exchangeable random network models for signed networks, where the degenerate unsigned version includes many commonly used network models as special cases [Nowicki and Snijders, 2001, Airolidi et al., 2008, Nickel, 2008, Hoff et al., 2002, Lei, 2021]. This flexibility is particularly preferred given the challenges in accurately modeling complex signed networks using simple parametric models. We first introduce a novel characterization of the generating process for infinitely exchangeable random network models for signed networks. Based on our findings, we propose a nonparametric graphon model for signed networks that is flexible to accommodate sparsity in both edge density and sign proportion. Under the proposed model for signed networks, we establish a non-asymptotic approximation to the distribution of a studentized ratio of the normalized count, and further construct valid confidence intervals based on this approximation.

We also apply our inference method to signed networks across various domains, including international relations in political science, protein-protein interactions in biology,

and both small- and large-scale social networks in social science. Our results reveal strong empirical evidence for balance theory, extending its applicability beyond its root domain in social psychology.

1.1 Related Works

The uncertainty quantification of the normalized count of balanced triangles has been studied under several balance-free models [Facchetti et al., 2011, Leskovec et al., 2010, Feng et al., 2022]. Among them, Facchetti et al. [2011] considered a balance-free model in which the edge signs are independently and identically distributed Bernoulli variables, with the probability equal to the fraction of negative edges in the observed network. Leskovec et al. [2010] employed a hypergeometric distribution corresponding to reshuffling edge signs while maintaining the fraction of observed negative edges. More recently, Feng et al. [2022] suggested a balance-free stratified model, where sign reshuffling occurs randomly across edges within the same embeddedness levels (*i.e.*, the number of triangles that an edge is part of), acknowledging the distinct behaviors of positive and negative edges. As far as we know, there is no consensus of the balance-free concept in the existing literature. Although the asymptotic properties of the normalized count under these balance-free models are useful for assessing whether or not a signed network is balance-free, they provide limited insight when the balance or weak balance is present in a signed network.

With a different primary focus of this paper, Jin et al. [2024b] studied signed cycle counts for two-sample binary network comparison. In particular, they constructed a signed network by differentiating two independent binary networks and developed test statistics based on the difference between the counts of balanced and unbalanced cycles of even length. Here, a cycle is defined as balanced if the product of its edge signs is positive, extending the concept of balance from triangles to cycles of any length. Under the assumption that both binary networks follow a degree-corrected mixture membership model [Zhang et al., 2020, Jin et al., 2024a] and that the probabilities of observing positive and negative signs are equal, they established the asymptotic normality of the test statistics. In contrast, our study focuses on assessing empirical evidence of balance theory by analyzing the count of balanced triangles of odd length under varying degrees of balance, where the results of Jin et al. [2024b] are not applicable.

We also note that our inference method is closely related to the line of work on network moment inference [Bhattacharyya and Bickel, 2015, Bickel et al., 2011, Thompson et al., 2016, Chen and Onnela, 2019, Levin and Levina, 2019, Green and Shalizi, 2022, Zhang and Xia, 2022, Lunde and Sarkar, 2022]. While several pioneering network bootstrap methods have been proposed for unsigned networks [Levin and Levina, 2019, Green and Shalizi, 2022, Bhattacharyya and Bickel, 2015], their justifications cannot be directly applied to our

setting. Among these methods, Levin and Levina [2019] developed a bootstrap procedure under the random dot-product graph (RDPG) model for inferring network quantities that can go beyond subgraph counts. However, it is unclear how to generalize the RDPG model for signed networks. Under the graphon model for unsigned networks, Bhattacharyya and Bickel [2015] and Green and Shalizi [2022] developed the node subsampling and the node resampling method respectively. Zhang and Xia [2022] established an explicit Edgeworth expansion formula that provides a higher-order accurate approximation of the distribution of a studentized network moment, compared to a simple normality approximation. In comparison to bootstrap-based methods, the empirical Edgeworth expansion is computationally more efficient. Given its merits, we extend the Edgeworth expansion method to our setting, leading to an inference method sharing the computation efficiency and higher-order accuracy. However, establishing the theoretical validity of our approach requires nontrivial efforts. Unlike the usual normalized count, where normalization is achieved by dividing by a fixed constant, our statistics involves the ratio of two network moments. In this case, the normalization denominator itself is a realization of random variables, which complicates the analysis of uncertain quantification. Furthermore, more precise conditions are necessary to account for the additional sparsity introduced by the sign proportion.

Notation We use “ $\stackrel{d}{=}$ ” to denote that two random objects have the same distribution. For two sequences $\{a_n\}$ and $\{X_n\}$, we write $X_n = O(a_n)$ or $X_n \preceq a_n$ if there exist constants C and $N > 0$ such that $|X_n| \leq Ca_n$ for all $n \geq N$. We write $X_n = o(a_n)$ or $X_n \prec a_n$ if $\lim_{n \rightarrow \infty} X_n/a_n = 0$, and $X_n \asymp a_n$ if $X_n \preceq a_n$ and $a_n \preceq X_n$. We define $X_n = \tilde{O}_p(a_n)$ if there exist constants C_1, C_2 and $N > 0$ such that $P(|X_n| \geq C_1 a_n) \leq C_2 n^{-1}$ for all $n \geq N$. We define $X_n = \omega(a_n)$ if for any real constant $C > 0$, there exists an integer constant N such that $X_n > Ca_n$ for every integer $n \geq N$.

2 Methodology

2.1 Exchangeable Random Network Model for Signed Networks

Exchangeable random network models represent a wide class of probabilistic models for network data, including the stochastic block model [Nowicki and Snijders, 2001], mixed-membership block model [Airoldi et al., 2008], random dot-product graph model [Nickel, 2008], and latent space model [Hoff et al., 2002]. The concept of node exchangeability involves viewing nodes as random samples and considering that the network distribution remains the same under any permutation of the nodes. For binary (unsigned) network data, the generating process for the infinitely exchangeable network model has been well studied [Orbanz and Roy, 2014] and serves as the theoretical foundation. Specifically, the

Aldous-Hoover theorem [Aldous, 1981, Hoover, 1979] says that any infinitely exchangeable random binary network can be generated by first sampling the nodal variables $\{X_i : i \geq 1\}$ independently from a uniform distribution on $[0, 1]$ and then independently of all others connecting each pair of nodes with probability $W(X_i, X_j)$, where $W(\cdot, \cdot) : [0, 1]^2 \rightarrow [0, 1]$ is a symmetric function. However, the corresponding process for signed networks remains unclear. Specifically, in an undirected signed network, each edge can take one of the three values $\{-1, 0, 1\}$.

To address this, we characterize the generating process for infinitely exchangeable random network models for signed networks and further propose a graphon model for sparse signed networks with finite network size. Consider a random two-way three-value symmetric array $\mathbf{A} = [A_{ij}]_{i,j \in \mathbb{N}}$ with $A_{ij} \in \{-1, 0, 1\}$ is row-column jointly exchangeable if

$$[A_{ij}]_{i,j \in \mathbb{N}} \stackrel{d}{=} [A_{\pi(i)\pi(j)}]_{i,j \in \mathbb{N}}$$

holds for any permutation mapping π on the finite indices, *i.e.*, for some $1 \leq j < j'$, $\pi(i) = i$ if $i \notin \{j, j'\}$, $\pi(j) = j'$ and $\pi(j') = j$. The following proposition states its equivalent representation and the corresponding generating process.

Proposition 1. *A random two-way array $\mathbf{A} = [A_{ij}]_{i,j \in \mathbb{N}}$ with $A_{ij} \in \{-1, 0, 1\}$ is row-column jointly exchangeable if and only if there exist two symmetric measurable functions $F(\cdot, \cdot) : [0, 1]^2 \rightarrow [0, 1]$ and $G(\cdot, \cdot) : [0, 1]^2 \rightarrow [0, 1]$ such that*

$$[A_{ij}]_{i,j \in \mathbb{N}} \stackrel{d}{=} [\mathbb{I}\{Y_{ij} < F(X_i, X_j)\}(-1)^{\mathbb{I}\{Y_{ij} > F(X_i, X_j)G(X_i, X_j)\}}]_{i,j \in \mathbb{N}},$$

where X_i and Y_{ij} , for $i, j \in \mathbb{N}$, are *i.i.d.* uniform random variables on $[0, 1]$. Here, $\mathbb{I}\{\cdot\}$ is the indicator function that equals 1 if the event holds and 0 otherwise. Therefore, the random two-way three-value array \mathbf{A} can be generated by the following process.

1. Generate $X_i \stackrel{i.i.d.}{\sim} U[0, 1]$ for $i \geq 1$;
2. For each pair (i, j) , independently sample $|A_{ij}| = 1$ with the probability $F(X_i, X_j)$ and otherwise $A_{ij} = 0$;
3. For each pair (i, j) with $|A_{ij}| = 1$, independently of all others, sample $A_{ij} = -1$ with the probability $G(X_i, X_j)$ and otherwise $A_{ij} = 1$.

Proposition 1 indicates that the distribution of \mathbf{A} is determined once the functions $F(\cdot, \cdot)$ and $G(\cdot, \cdot)$ are specified, with the proof provided in the Supplemental Materials. Motivated by Proposition 1, we propose a nonparametric graphon model for undirected signed networks with n nodes. Denote the corresponding signed symmetric adjacency matrix by $A = [A_{ij}] \in \{-1, 0, 1\}^{n \times n}$. Specifically, $A_{ij} = 1$ indicates a positive edge

between the nodes i and j , $A_{ij} = -1$ indicates a negative edge, and $A_{ij} = 0$ indicates no edge between nodes i and j . The following graphon model is governed by two symmetric measurable functions $F : [0, 1]^2 \rightarrow [0, 1]$ and $G : [0, 1]^2 \rightarrow [0, 1]$ as well as two additional sparsity parameters, ρ_n and $s_n \in (0, 1)$.

Definition 1 (Graphon Model for Signed Networks $\mathcal{G}(n, F, G, \rho_n, s_n)$). *For $1 \leq i \leq n$, let $X_i \sim U[0, 1]$ be the latent variables independently sampled from the uniform distribution. Conditional on the latent variables of two nodes i and j , an edge between two nodes is independently drawn with probability $\rho_n F(X_i, X_j)$, i.e.,*

$$pr(|A_{ij}| = 1 \mid X_i, X_j) = \rho_n F(X_i, X_j), \quad \text{for all } 1 \leq i < j \leq n;$$

then for each edge (i.e. $|A_{ij}| = 1$), independently of all others, it takes the negative sign with probability $s_n G(X_i, X_j)$ and the positive sign otherwise, i.e.,

$$pr(A_{ij} = -1 \mid |A_{ij}| = 1, X_i, X_j) = s_n G(X_i, X_j), \quad \text{for all } 1 \leq i < j \leq n.$$

Besides, $A_{ij} = A_{ji}$ for all $i \neq j$ and $A_{ii} = 0$. We write $A \sim \mathcal{G}(n, F, G, \rho_n, s_n)$ to denote a signed network with n nodes generated from the above procedure.

For identifiability, we constrain the integral of F and G over $[0, 1]^2$ being constants while allowing ρ_n and s_n to change with the network size n . In particular, ρ_n and s_n specify the network edge density and the proportion of negative signs among all edges, respectively. Given that negative edges are less common than positive edges in real-world networks, we focus on the case $s_n = o(1)$ to establish the theoretical results in Section 3. Nonetheless, when negative edges are more prevalent, our proposed inference method and its theoretical validity still hold by considering $pr(A_{ij} = 1 \mid |A_{ij}| = 1, X_i, X_j) = s_n G(X_i, X_j)$.

2.2 Population Parameters for Balance and Inference Procedure

To measure the overall degree of balance, we aim to make inference for the expected proportion of balanced triangles among all triangles in a signed network. This population parameter is defined by

$$w_n = pr(h_{\blacktriangle}(A_{i,j,k}) = 1 \mid |h_{\Delta}(A_{i,j,k}) = 1),$$

where $h_{\Delta}(A_{i,j,k})$ and $h_{\blacktriangle}(A_{i,j,k})$ are indicator functions for the events where nodes i, j and k form a triangle and a balanced triangle, respectively. Without loss of generality, we use $\{i, j, k\}$ to index any three nodes in a network $A \sim \mathcal{G}(n, F, G, \rho_n, s_n)$. This population parameter does not rely on specific indexes due to node exchangeability. A higher value

of w_n indicates stronger evidence of balance theory. In addition, motivated by weak balance theory, we define more granular population parameters that describe the expected proportion of each type of triangle:

$$w_{n,t} = \text{pr}(h_t(A_{i,j,k}) = 1 \mid |h_\Delta(A_{i,j,k}) = 1), \text{ for } 1 \leq t \leq 4,$$

where $h_t(A_{i,j,k})$ is the indicator function for the event where nodes i, j and k form a type- t triangle. In particular, a smaller value of $w_{n,2}$ indicates stronger evidence of the weak balance theory.

Next, we develop a computationally efficient procedure to construct confidence intervals for population parameters, with its theoretical validity established under the proposed graphon model in Section 3. For the sake of space, we illustrate the proposed inference procedure by detailing the derivation of a confidence interval for w_n . The procedure for deriving confidence intervals for $w_{n,t}$ is similar to that for w_n and is therefore omitted. We start with the normalized count and study its studentization. This approach is motivated by the observation that studentization leads to higher-order accurate approximations in i.i.d. data [Wasserman, 2006] and unsigned network data [Zhang and Xia, 2022]. Define the two sample network moments as

$$\widehat{U}_n = \sum_{1 \leq i_1 < i_2 < i_3 \leq n} h_\blacktriangle(A_{i_1, i_2, i_3}) / C_n^3, \quad \widehat{V}_n = \sum_{1 \leq i_1 < i_2 < i_3 \leq n} h_\Delta(A_{i_1, i_2, i_3}) / C_n^3,$$

and their population versions by $u_n = \mathbb{E}\{h_\blacktriangle(A_{1,2,3})\}$ and $v_n = \mathbb{E}\{h_\Delta(A_{1,2,3})\}$, respectively. It follows that $w_n = u_n/v_n$. The normalized count is the ratio of these two sample network moments. To proceed, we analyze its studentized version $\widehat{T}_n := (\widehat{U}_n/\widehat{V}_n - u_n/v_n)/\widehat{S}_n$, where the design of an analytically tractable variance estimator, \widehat{S}_n , will be specified later. We then obtain a high-order accurate approximation G_n (defined in Theorem 1) to the cumulative distribution function (CDF) of \widehat{T}_n . Finally, we use the empirical version \widehat{G}_n to construct the confidence interval for w_n . In contrast to bootstrap-based methods, the computational cost of calculating \widehat{G}_n given the explicit formula is comparable to that of using a simple normal approximation.

To derive the variance estimator, we decompose the numerator of \widehat{T}_n , which is $\widehat{U}_n/\widehat{V}_n - u_n/v_n$, by introducing intermediate terms $U_n = \mathbb{E}(\widehat{U}_n \mid X_1, \dots, X_n)$ and $V_n = \mathbb{E}(\widehat{V}_n \mid X_1, \dots, X_n)$. The stochastic variation arises from both the randomness in the latent variables $\{X_i\}_{i=1}^n$ and the categorical distribution of $A_{ij} \in \{0, \pm 1\}$ given $\{X_i\}_{i=1}^n$. We further decompose $U_n - u_n$ and $V_n - v_n$ using Hoeffding's decomposition [Hoeffding, 1992]. Specifically, we have $U_n - u_n = 3 \sum_{i=1}^n g_1(X_i)/n + 6 \sum_{1 \leq i < j \leq n} g_2(X_i, X_j)/\{n(n-1)\} + \text{remainder}$, where $g_1(x_1) := \mathbb{E}\{h_\blacktriangle(X_1, X_2, X_3) \mid X_1 = x_1\} - u_n$ and $g_2(x_1, x_2) := \mathbb{E}\{h_\blacktriangle(X_1, X_2, X_3) \mid$

$X_1 = x_1, X_2 = x_2\} - u_n - \sum_{1 \leq i \leq 2} g_1(x_i)$. Here, we define $h_{\blacktriangle}(X_1, X_2, X_3) := \mathbb{E}\{h_{\blacktriangle}(A_{1,2,3}) \mid X_1, X_2, X_3\}$ and the remainder term is of a smaller order compared to the leading terms. Similarly, we denote the terms in Hoeffding's decomposition for $V_n - v_n$ by f replacing g . The following proposition gives the leading order of $\text{var}(\widehat{U}_n/\widehat{V}_n - u_n/v_n)$, with the proof provided in the Supplemental Materials.

Proposition 2. *Assuming the conditions in Theorem 1 (specified later) hold, we have:*

$$\lim_{n \rightarrow \infty} \mathbb{E} \left[9 \left\{ g_1(X_1)/v_n - u_n f_1(X_1)/v_n^2 \right\}^2 / n \right] / \text{var}(\widehat{U}_n/\widehat{V}_n - u_n/v_n) = 1. \quad (1)$$

Based on Equation (1), we propose the variance estimator:

$$n\widehat{S}_n^2 = \frac{9}{n} \sum_{i=1}^n \left[\sum_{\substack{1 \leq i_1 < i_2 \leq n \\ i_1, i_2 \neq i}} \left\{ h_{\blacktriangle}(A_{i,i_1,i_2})/\widehat{V}_n - \widehat{U}_n h_{\Delta}(A_{i,i_1,i_2})/\widehat{V}_n^2 \right\} / C_{n-1}^2 \right]^2.$$

3 Theoretical Results

The validity of the proposed inference procedure relies on establishing an accurate approximation of the distribution function of \widehat{T}_n , denoted by $F_{\widehat{T}_n}(\cdot)$. Edgeworth expansion provides a higher-order approximation of a distribution compared to the simple normality approximation [Edgeworth, 1883, Wallace, 1958, Bentkus et al., 1997, Hall, 2013], and has been widely applied to studentized or standardized U-statistics [Callaert et al., 1980, Callaert and Veraverbeke, 1981, Bickel et al., 1986, Zhang and Xia, 2022]. The empirical Edgeworth expansion was later established by Putter and van Zwet [1998] and Helmers [1991]. Before presenting our Edgeworth expansion formula, we introduce some notation for simplicity. Define $p_1(X_i) = f_1(X_i)/v_n$, $q_1(X_i) = g_1(X_i)/v_n - u_n f_1(X_i)/v_n^2$, $q_2(X_i, X_j) = g_2(X_i, X_j)/v_n - u_n f_2(X_i, X_j)/v_n^2$, and $\xi_1^2 = \mathbb{E}\{q_1^2(X_1)\}$. Let σ_n^2 denote the leading term of $\text{var}(\widehat{U}_n/\widehat{V}_n - u_n/v_n)$ as specified in Proposition 2 and it follows that $\sigma_n^2 = 9\xi_1^2/n$. Following Shao et al. [2022], we introduce an artificial Gaussian random variable to bypass Cramér's condition, which is typically assumed in the analysis of Edgeworth expansion for U-statistics. Let $\delta_T \sim N(0, c_\delta \cdot n^{-1} \log n)$ be a Gaussian variable independent of the observed signed network A , with a sufficiently large constant c_δ . We use $\widehat{T}_n + \delta_T$ rather than \widehat{T}_n for inference. The following theorem characterizes the Edgeworth expansion approximation for $F_{\widehat{T}_n + \delta_T}(\cdot)$, with a deviation bounded by $\mathcal{E}(n, s_n, \rho_n) := n^{-1} \rho_n^{-3/2} \log^{3/2} n (1 + s_n \log n) + n^{-1} s_n^{-1/2} \rho_n^{-1/2}$ under mild conditions.

Theorem 1. *Define the population Edgeworth expansion as*

$$G_n(x) = \Phi(x) + \phi(x) \{a(x^2/3 + 1/6) + b(x^2 + 1) - 3cx^2\} / \sqrt{n},$$

where $\phi(\cdot)$ and $\Phi(\cdot)$ are the density and distribution functions of the standard normal distribution respectively, the coefficients are given by $a = \mathbb{E}\{q_1^3(X_1)\}/\xi_1^3$, $b = \mathbb{E}\{q_1(X_1)q_1(X_2)q_2(X_1, X_2)\}/\xi_1^3$, $c = \mathbb{E}\{q_1(X_1)p_1(X_1)\}/\xi_1$. If the following conditions hold: (a) $F(\cdot, \cdot)$, $G(\cdot, \cdot) > C_1$ for some constant $C_1 > 0$; (b) $n\sigma_n^2 > C_2$ for some constant $C_2 > 0$; (c) $s_n^2 \rho_n^3 \succeq n^{-2} \log^8 n$, $s_n \prec 1$ and $\rho_n \succ n^{-1/2}s_n$, we have

$$\|F_{\widehat{T}_n + \delta_T}(x) - G_n(x)\|_\infty = O(\mathcal{E}(n, s_n, \rho_n)).$$

The regularity Condition (a) ensures that the probabilities of having an edge and a negative sign are of the order ρ_n and s_n , respectively. Condition (b) is a non-degeneration assumption that has been similarly made in the literature [Zhang and Xia, 2022, Shao et al., 2022]. This implies that the variance of $q_1(X_i)$ is positively lower-bounded. Condition (c) specifies the feasible range for network edge sparsity and the proportion of negative signs. Specifically, $s_n^2 \rho_n^3$ corresponds to the order of the probability of observing a type-3 balanced triangle. When we replace $\rho_n \succ n^{-1/2}s_n$ in Condition (c) with a stronger condition $\rho_n^3 = w(n^{-1})$, our Edgeworth expansion yields higher-order accuracy compared to a simple normal approximation. This sparsity condition $\rho_n^3 = w(n^{-1})$ aligns with those made in the existing literature on network moment inference [Bhattacharyya and Bickel, 2015, Bickel et al., 2011, Zhang and Xia, 2022].

The above population Edgeworth expansion still involves coefficients that depend on the unknown underlying data-generating distribution. We define an empirical Edgeworth expansion by replacing the unknown coefficients with their empirical estimates. The following theorem establishes the approximation error of the empirical Edgeworth expansion to the CDF of $\widehat{T}_n + \delta_T$.

Theorem 2. *Define the empirical Edgeworth expansion as*

$$\widehat{G}_n(x) = \Phi(x) + \phi(x) \left\{ \widehat{a}(x^2/3 + 1/6) + \widehat{b}(x^2 + 1) - 3\widehat{c}x^2 \right\} / \sqrt{n},$$

where \widehat{a} , \widehat{b} and \widehat{c} are the empirical estimates of a , b and c , respectively. The detailed formulas are given by (D.1) in the Supplemental Materials. Assuming the conditions in Theorem 1 hold, we have

$$\|F_{\widehat{T}_n + \delta_T}(x) - \widehat{G}_n(x)\|_\infty = \widetilde{O}_p(\mathcal{E}(n, s_n, \rho_n)).$$

Theorem 2 indicates that the maximum deviation of the empirical Edgeworth expansion from the CDF of \widehat{T}_n over the support is bounded by $\mathcal{E}(n, s_n, \rho_n)$ with high probability (at least $1 - n^{-1}$). Consequently, this result can be used to construct a Cornish-Fisher confidence interval with a provable coverage probability as follows.

Corollary 1. For any $\alpha \in (0, 1)$, we define

$$\widehat{q}_{\widehat{T}_{n;\alpha}} := z_\alpha - \{\widehat{a}(z_\alpha^2/3 + 1/6) + \widehat{b}(z_\alpha^2 + 1) - 3\widehat{c}z_\alpha^2\}/\sqrt{n} - \delta_T,$$

where $z_\alpha := \Phi^{-1}(\alpha)$ and \widehat{a} , \widehat{b} and \widehat{c} are given by (D.1) in the Supplemental Materials. Assuming the conditions in Theorem 1 hold, the two-sided confidence interval for w_n ,

$$(\widehat{U}_n/\widehat{V}_n - \widehat{q}_{\widehat{T}_{n;1-\alpha/2}} \cdot \widehat{S}_n, \widehat{U}_n/\widehat{V}_n - \widehat{q}_{\widehat{T}_{n;\alpha/2}} \cdot \widehat{S}_n),$$

has a $1 - \alpha + O(\mathcal{E}(n, s_n, \rho_n))$ coverage probability.

Remark 1. Note that the Edgeworth expansion approximation in Theorem 2 can also be used to perform both two-sided or one-sided test. To illustrate, consider testing a balance-free null value with the hypothesis

$$H_0 : w_n = c_n \quad \text{vs} \quad H_1 : w_n > c_n.$$

The null value c_n can be derived from various balance-free models. For example, the null model in Facchetti et al. [2011] assumes that the edge signs are i.i.d. Bernoulli variables, with probability equal to the fraction of negative edges in the observed network. Our null hypothesis accommodates this scenario by setting $c_n = (1 - s_n)^3 + 3s_n^2(1 - s_n)$. Similarly, in Jin et al. [2024b], the balance-free null model assumes equal probabilities for positive and negative edges, which our null hypothesis reflects by setting $c_n = 0.5$. Using our empirical Edgeworth expansion formula, we evaluate the empirical p-value $\widehat{p} := \widehat{G}_n((\widehat{U}_n/\widehat{V}_n - c_n)/\widehat{S}_n)$. Following Zhang and Xia [2022], given a significance level α , we reject the null hypothesis H_0 if $\widehat{p} < \alpha$. The higher-order accuracy of our Edgeworth expansion allows us to control the Type-I error at $\alpha + O(\mathcal{E}(n, s_n, \rho_n))$ and the type-II error at $o(1)$ when $|w_n - c_n| = \omega(n^{-1/2})$.

Remark 2. The inference procedure described above and its theoretical validity can be adapted to analyze each of the four types of triangles within the network, thereby providing detailed insights into specific patterns. For example, a lower proportion of type-2 triangles suggests strong evidence of weak balance in the network. For each type of triangle, we construct a studentized ratio of sample network moments and establish an Edgeworth expansion to approximate the CDF of this studentized ratio. The corresponding approximation error bounds are provided in the Supplemental Material.

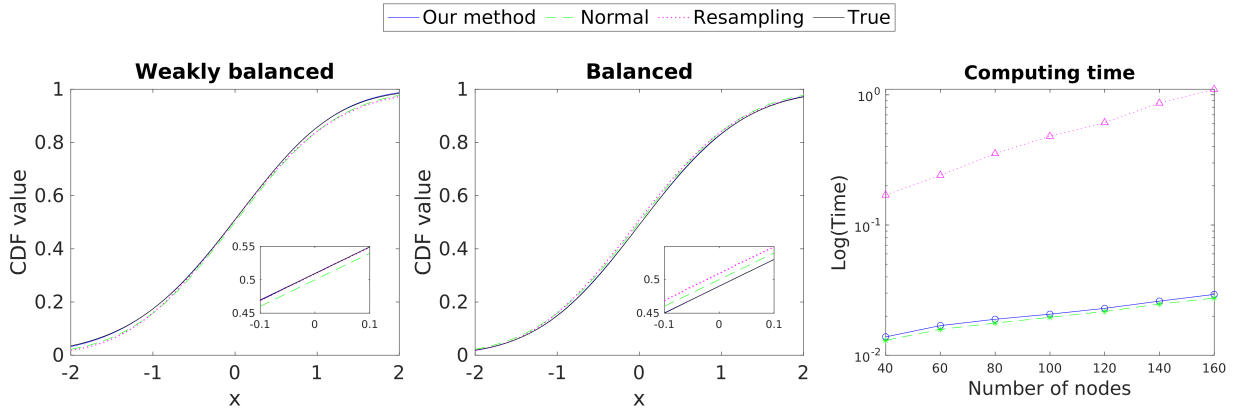


Figure 2: The true CDF of the studentized ratio of network moments, along with its approximations (including our empirical Edgeworth expansion formula, standard normal approximation, and the bootstrap-based node-resampling method), is displayed on the left for balanced triangles and in the middle for type-2 triangles, respectively. On the right, we provide a comparison of the computing time for each approximation method.

4 Simulation Studies

4.1 Comparative Analysis of CDF Approximations and their Computational Efficiency

We begin by assessing the accuracy and computational efficiency of approximations for the CDF of the studentized ratio of network moments. We compare our empirical Edgeworth expansion approach with two methods - the standard normal approximation and bootstrap-based node resampling method. Note that the node resampling method [Green and Shalizi, 2022], originally developed for unsigned network moments, cannot be directly applied in our context. We adapt it to enable inference for the expected proportion of each type of triangle, with detailed procedure provided in the Supplementary Material.

To compare their approximations to the true CDF, we generate signed networks with $n = 160$ nodes from the graphon model defined by the functions $\rho_n F(x, y) = 0.8$ and $s_n G(x, y) = 2 \cos(x^2 + y^2)/3 + 0.3$. To evaluate the true CDF of \widehat{T}_n , we generate a large sample of $N = 10^6$ networks from the graphon model. The adapted node-resampling method approximates the CDF by resampling $B = 10^5$ networks from the estimated graphon functions. For the sake of space, we present the results for the population parameters for balance (*i.e.*, w_n) and weak balance (*i.e.*, $w_{n,2}$) in the main text, while the full results for other types of triangles are provided in the Supplemental Material. The left and middle panels of Figure 2 suggest our method closely aligns with the true CDFs, offering a better approximation compared to the normal approximation and the resampling method.

To further compare computational efficiency, we vary the network size from 40 to 160.

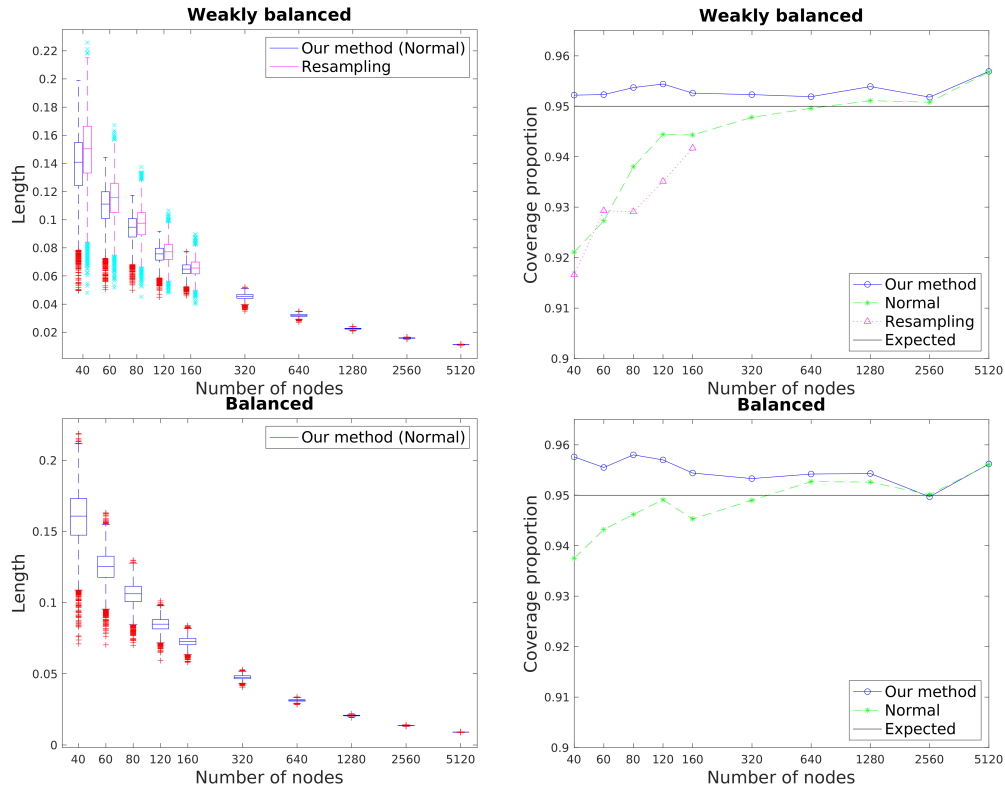


Figure 3: The length and coverage proportion of 95% confidence intervals for (weakly) balanced triangles in relation to varying network size are presented from left to right, respectively.

The right panel of Figure 2 summarizes the logarithm of computing time relative to the network size. It shows that our Edgeworth expansion approach and the normal approximation are computationally more efficient than the node-resampling method. The former two use explicit formulas, where the primary computational cost is a few matrix multiplications to calculate the studentized statistics, while the latter necessitates a large number of bootstrap replications. Overall, our method, with a computational cost identical to the simple normal approximation, provides higher-order accuracy, as demonstrated in Figure 2.

4.2 Impact of Network Size and Sparsity

In this subsection, we evaluate the coverage proportion and the length of confidence intervals (CIs) constructed by each method and investigate the impact of the network size and sparsity on their effectiveness. We generate networks using the same graphon model described in Section 4.1. Hereafter, we conduct 10,000 replications for each setting.

We first vary the network size with a range of exponentially increasing set $\{40, 80, \dots, 5120\}$. For large sizes $n \in \{320, 640, \dots, 5120\}$, due to the high computational cost of the node-resampling method, we only compare our method with the standard normal approximation.

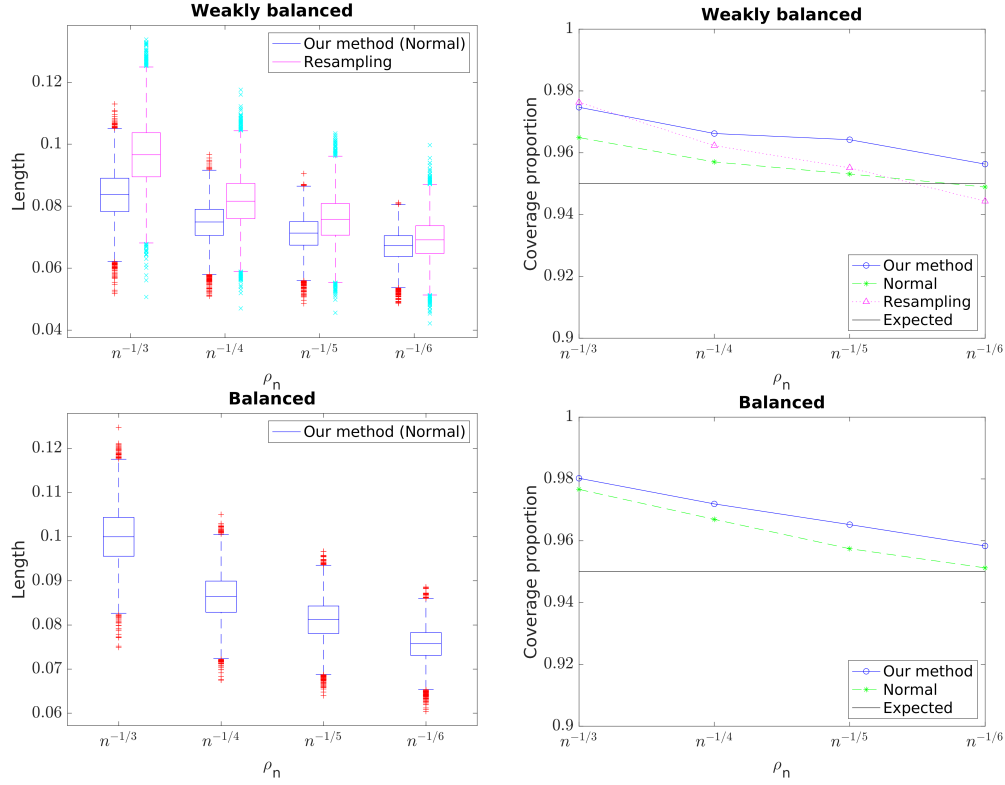


Figure 4: The length and coverage proportion of 95% confidence intervals for (weakly) balanced triangles in relation to varying network sparsity are presented from left to right, respectively.

Figure 3 summarizes the performance of 95% CIs for w_n and $w_{n,2}$ with respect to varying network sizes. Our method consistently achieves proper coverage across different network sizes. For smaller networks, our method obtains higher coverage than the normal and node resampling methods, which highlights the advantage of achieving higher-order approximation to the CDF. The CI length for all methods decreases as the network size increases, with our method and the normal approximation slightly outperforming the resampling method in terms of shorter lengths. Note that our method always yields a CI length identical to that of the normal approximation, so we only plot one in the figure.

Furthermore, we set $n = 160$ and vary ρ_n with a range of $\{n^{-1/3}, n^{-1/4}, n^{-1/5}, n^{-1/6}\}$, which leads to the network density ranging across 18.4%, 26.4%, 33.6% and 52.0%. Figure 4 summarizes the effectiveness of 95% CIs for w_n and $w_{n,2}$ with respect to varying network sparsity. We can see that all methods achieve reasonable coverage proportions across varying network sparsity, and the CI length of our method and the normal approximation consistently remains shorter than that of the resampling method. As the network density increases, the CI length decreases and the coverage proportion approaches the nominal level 95%. This is attributed to the increasing number of observed signs as the network becomes denser.

4.3 Varying Degree of Balance

Finally, we investigate the performance of our inference method across various extent of balance. To this end, we generate networks with $n = 160$ nodes from the graphon model defined by $s_n G(x, y; \alpha) = 1/(1 + \exp(\alpha \cdot (x - 0.4)(y - 0.4)))$. Here, α controls the overall degree of balance. Specifically, when $\alpha = 0$, each edge is equally likely to be positive or

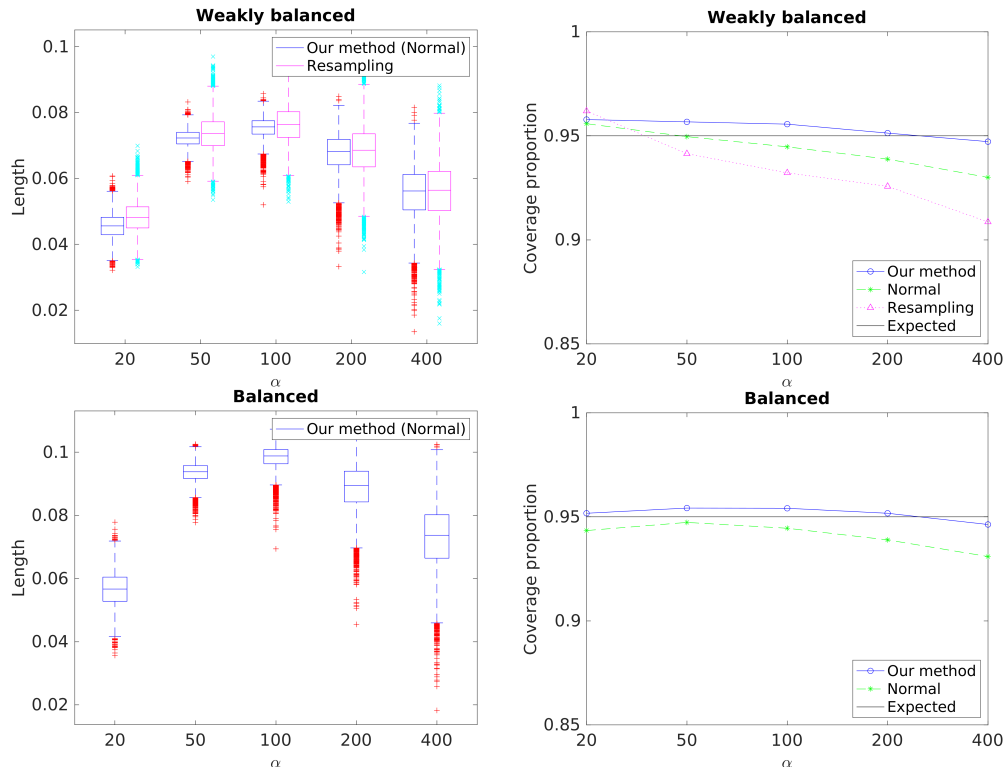


Figure 5: The length and coverage proportion of 95% confidence intervals of (weakly) balanced triangles in relation to varying degree of balance are presented from left to right, respectively.

negative, considered as a balance-free case. As α approaches infinity, the edge signs follow a block model with membership probabilities $\pi = (0.4, 0.6)$. In particular, edges tend to have positive signs within blocks and negative signs between them, leading to balanced triangles. Therefore, a larger α corresponds to a greater degree of balance.

We vary α from $\{20, 50, 100, 200, 400\}$, with the proportion of balanced triangles increasing from 59.0% to 92.6%. The proportion of each type of triangle is provided in Figure S4, showing an increase in balanced triangles (types 1 and 3) and a decrease in unbalanced triangles (types 2 and 4). As indicated in Figure 5, our method consistently maintains proper coverage proportions across varying extent of balance. Notably, when α is large, *i.e.*, a great extent of balance is present, our method achieves more stable coverage proportion compared to both the normal approximation and the resampling method.

5 Real-world Data Examples

5.1 Problem Setup

In this section, we apply the proposed method to analyze the evidence of balance and weak balance in real-world signed networks across various fields. A higher expected proportion of balanced triangles, *i.e.*, w_n , indicates stronger evidence of balance, while a lower expected proportion of type-2 triangles, *i.e.*, $w_{n,2}$, suggests the weak balance. To measure the degree of balance in an observed signed network, we establish 95% confidence intervals for w_n and $w_{n,2}$, and compare them with balance-free baselines. Specifically, we consider two balance-free models to compute the corresponding expected proportions as baselines. The first model assumes that each edge has an equal probability of being positive or negative, setting baseline values as 0.5 for balanced triangle and 0.25 for type-2 triangle. We refer to them as “Baseline 50%” and “Baseline 25%” respectively below. This baseline aligns with the concept of the population-level balance introduced in Tang and Zhu [2024], where a signed network is considered population-level balanced if the expected proportion of balanced triangles exceeds 0.5. The second model adjusts for the proportion of negative edges [Facchetti et al., 2011]. Here, edge signs are independently and identically distributed Bernoulli variables, with the probability equal to the fraction of negative edges in the observed network. We refer to the second baseline as “Adjusted Baseline”. Details on calculating these baselines and the results for other types of triangles are provided in the Supplemental Materials.

5.2 International Relation Network

We apply our method to international relation networks with 217 countries from 1910 to 1945, sourced from the Correlates of War project [Gibler, 2008, Palmer et al., 2022]. For each five-year period, we construct a signed network. We define a positive edge for a pair of countries if the duration of alliance agreements exceeds that of militarized disputes; a negative edge if the duration of disputes exceeds that of alliance agreements; and no edge if there was no relationship. Figure 6a reports the network size and the numbers of positive and negative edges for each five-year signed network. In particular, the number of negative edges substantially increases during World War I (1914-1918) and II (1939-1945).

We summarize the confidence intervals for the expected proportion of balanced triangles in Figure 6b. Compared to two baselines, the 95% confidence intervals for w_n are above the baseline values for all time frames except from 1936 to 1940. This finding provides strong evidence supporting the structural balance theory over most time frames, suggesting that countries tend to form balanced triadic relationships in the international relation

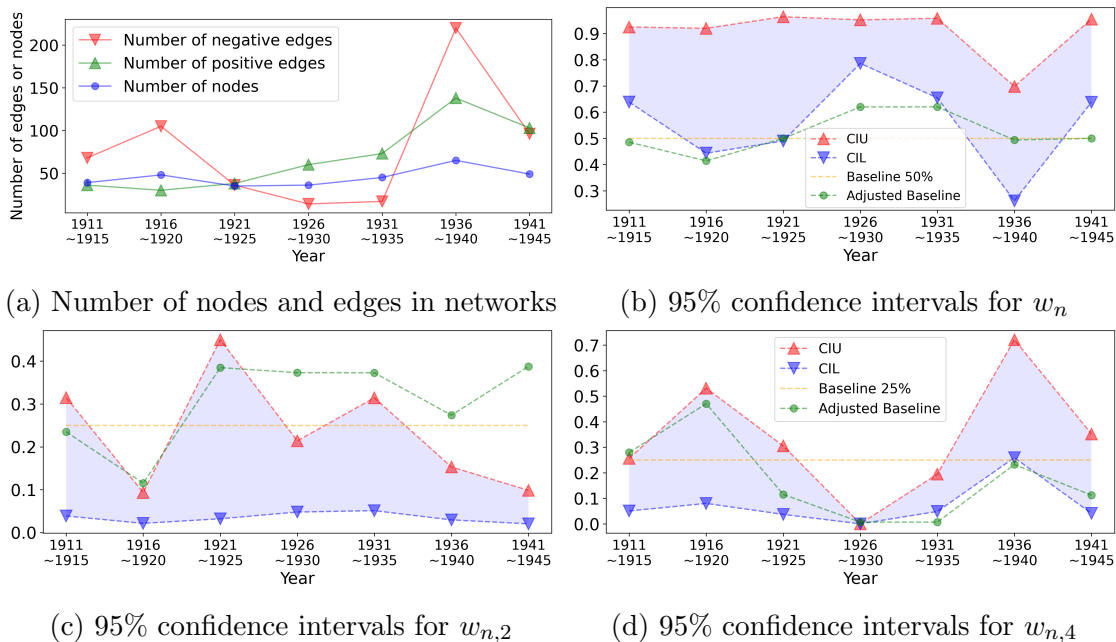
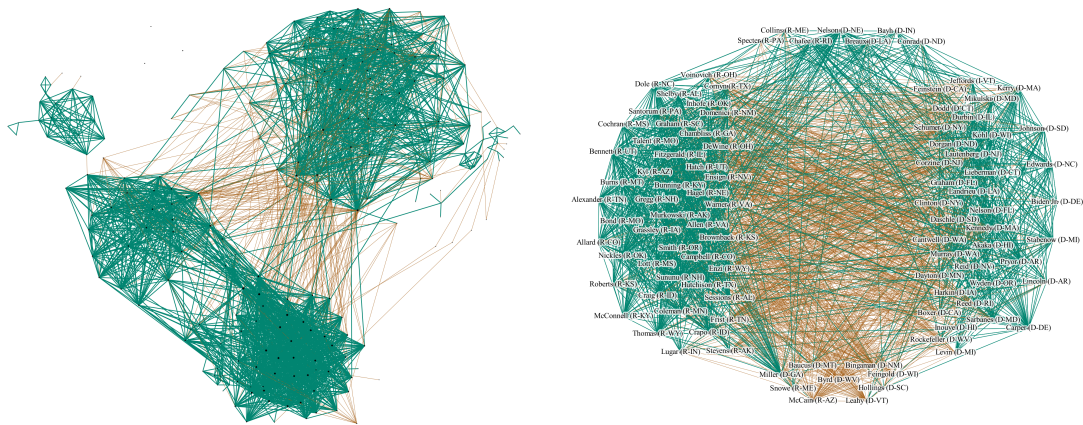


Figure 6: (a) The network size and the number of positive and negative edges for each five-year signed network from 1911 to 1945; (b) The 95% confidence intervals for the expected proportion of balanced triangles, i.e., w_n ; (c) The 95% confidence intervals for the type-2 triangle, i.e., $w_{n,2}$; (d) The 95% confidence intervals for the type-4 triangle, i.e., $w_{n,4}$. For (b)-(d), the red upper triangle represents the upper bound of confidence intervals; the blue lower triangle represents the lower bound of confidence intervals; and the yellow and green dashed lines represent baselines under two balance-free models.

network. However, during the 1936-1940 period, we observe an obvious deviation from the general trend. The confidence interval for the type-4 triangle is notably high, as shown in Figure 6d, indicating that hostility often exists among countries during this time frame. This observation may be attributed to the full-scale outbreak of World War II, with increasing tensions and the emergence of conflicts. While the network lacks strong structural balance during this time, it still maintains a degree of weak balance when considering only type-2 triangles as unbalanced. As illustrated in Figure 6c, the confidence interval for the proportion of type-2 triangles is much below the baseline values.

5.3 Protein-Protein Interaction Network

Linking physical and functional associations among proteins is useful for understanding how their interactions relate to cellular function and viability. In particular, Huttlin et al. [2021] integrated BioPlex networks [Huttlin et al., 2015] in 293T and HCT116 cells with genome-wide CRISPR co-essentiality profiles from Project Achilles [Meyers et al., 2017]. They calculated the functional similarity between fitness profiles for each interacting protein pair using Spearman’s correlation coefficient, which can be either positive or negative. Their



(a) Protein-protein interaction network

(b) 108th U.S. Senate network

Figure 7: Visualization of two networks: (a) the functional similarity network among interacting proteins, where proteins with more than 25 edges are plotted, and (b) the network among U.S. senators. In both networks, green edges represent positive interactions and red edges represent negative interactions.

findings indicate that these positive and negative correlations reflect different structural relationships, highlighting the importance of differentiating between signs of functional similarity.

To investigate this further, we construct a signed network among proteins by retaining only significant correlations between fitness profiles. Specifically, we assign a positive edge between a pair of interacting proteins if the p-value associated with Spearman’s correlation is less than 0.05 and the correlation is positive. We assign a negative edge if the significant correlation is negative. No edge is assigned for non-significant correlations or non-interacting pairs. We then apply our inference method to this signed network and summarize the results in Table 1. The confidence interval for w_n is significantly above the baseline value, providing strong evidence of network balance. Compared to the international relation network, the confidence intervals in this PPI network are much shorter due to its larger network size.

We visualize the signed PPI network in Figure 7a, where we observe several clusters of nodes. There are more connections within clusters and fewer edges between clusters. Particularly, the edges between the upper-right cluster and the others are mostly negative, while edges within or between other clusters are mostly positive. This observation aligns with the population-level balance structure identified by Tang and Zhu [2024], where node communities can be merged into two groups where edges are predominantly positive within groups and negative between groups. Notably, Huttlin et al. [2021] observed that positively

correlated proteins typically belong to the same complexes, whereas negatively correlated proteins belong to different complexes and exhibit antagonistic interactions. The balance structure provides insight into the functional organization of protein interactions, supporting the observation that proteins within the same complex tend to cooperate, while those in different complexes may have opposing functions.

Datasets	Protein-Protein	U.S.Senate	Wikipedia Elections
Nodes $[n]$	8777	100	7115
Edges	6.05×10^{-4}	0.40	3.98×10^{-3}
Negative Signs	0.31	0.42	0.22
Type-1	0.891	0.490	0.659
Type-2	0.019	0.031	0.230
Type-3	0.089	0.410	0.096
Type-4	0.001	0.069	0.015
CI for w_n	(0.968, 0.989)	(0.792, 0.943)	(0.728, 0.780)
Adjusted Baseline for w_n	0.529	0.502	0.587

Table 1: Characteristics of real-world signed networks, including the number of nodes, the proportion of edges, the proportion of negative signs, the proportion of type- t triangles for $1 \leq t \leq 4$, 95% confidence intervals for w_n , and the adjusted balance-free baseline for w_n .

5.4 Social Networks

Finally, we apply our method to two social networks where balance theory originates: a small-scale U.S. Senate network [Fowler, 2006] and a large-scale Wikipedia Elections network [Leskovec et al., 2010]. The first signed network among U.S. senators is constructed using Fowler’s Senate bill co-sponsorship data [Fowler, 2006]. A positive edge is assigned between two senators if they co-sponsored bills significantly more frequently than expected, suggesting a political alliance. Conversely, a negative edge is assigned if they co-sponsored bills significantly less frequently than expected. Detailed information on the network construction is provided in the Supplemental Materials. This signed network consists of 100 senators as nodes, with 1,164 positive edges and 835 negative edges. The second large-scale signed network among Wikipedia users is based on their votes for or against the promotion of other users to administrator status [Leskovec et al., 2010]. We analyze an undirected version of the dataset, which includes 7,115 Wikipedia users, with 78,440 positive edges and 22,253 negative edges.

We apply the inference method to these two social networks, and our results in Table 1 show strong evidence of balance in both cases. The confidence intervals for the expected proportion of balanced triangles are all above the balance-free baselines. In particular, as shown in Figure 7b, the U.S. Senate network consists of two major clusters, which mostly align with the Democratic and Republican parties. Within each cluster, most connections

are positive; in contrast, the connections between the two clusters are mostly negative. This may be attributed to that senators within each cluster co-sponsor bills proposed by their members and in most cases do not support bills from the other cluster. This partition structure aligns with the concept of balance theory.

6 Discussions

In this work, we have introduced a nonparametric inference method to measure the overall degree of balance in signed networks. Under the proposed node-exchangeable graphon model for signed networks, we construct confidence intervals for the population parameters characterizing balance and weak balance. We have established the coverage guarantee of our method across varying degrees of balance. The proposed inference procedure is as computationally efficient as a simple normal approximation while offering a higher-order approximation. Additionally, we have applied our method to evaluate empirical evidence of balance in various real-world signed networks, where our results indicate strong evidence of balance in most networks examined.

Our empirical findings highlight the importance of sign information and the necessity of incorporating balance into statistical modeling for future work. Notably, in the protein-protein interaction network, we observed a high proportion of balanced triangles. We conjecture that this observation may be common in network data constructed by computing pairwise correlations from nodal measurements, such as neuron-neuron and gene-gene interactions [Zalesky et al., 2012, Xia et al., 2013, Greene et al., 2015, Wang et al., 2018]. Exploring the application of balance theory for more efficient statistical analysis in these contexts is an intriguing direction for future work.

In this work, we focus on inferring the degree of balance within time-static signed networks. However, the core principle of balance theory is its tendency to avoid conflicts that might destabilize the system, inherently moving towards a more balanced state. An interesting direction for future research is to develop inference tools for balance in the context of dynamic signed networks.

References

- Edo M Airoldi, David Blei, Stephen Fienberg, and Eric Xing. Mixed membership stochastic blockmodels. *Advances in Neural Information Processing Systems*, 21, 2008.
- David J Aldous. Representations for partially exchangeable arrays of random variables. *Journal of Multivariate Analysis*, 11(4):581–598, 1981.

- Vidmantas Bentkus, Friedrich Götze, and Willem R van Zwet. An edgeworth expansion for symmetric statistics. *The Annals of Statistics*, 25(2):851–896, 1997.
- Sharmodeep Bhattacharyya and Peter J. Bickel. Subsampling bootstrap of count features of networks. *The Annals of Statistics*, 43(6):2384 – 2411, 2015. doi: 10.1214/15-AOS1338. URL <https://doi.org/10.1214/15-AOS1338>.
- Peter J. Bickel, Aiyou Chen, and Elizaveta Levina. The method of moments and degree distributions for network models. *The Annals of Statistics*, 39(5):2280 – 2301, 2011. doi: 10.1214/11-AOS904. URL <https://doi.org/10.1214/11-AOS904>.
- PJ Bickel, Friedrich Götze, and WR Van Zwet. The edgeworth expansion for u-statistics of degree two. *The Annals of Statistics*, pages 1463–1484, 1986.
- Herman Callaert and Noel Veraverbeke. The order of the normal approximation for a studentized u-statistic. *The Annals of Statistics*, pages 194–200, 1981.
- Herman Callaert, Paul Janssen, and Noel Veraverbeke. An edgeworth expansion for u-statistics. *The Annals of Statistics*, pages 299–312, 1980.
- Dorwin Cartwright and Frank Harary. Structural balance: a generalization of heider’s theory. *Psychological Review*, 63(5):277, 1956.
- Sixing Chen and Jukka-Pekka Onnela. A bootstrap method for goodness of fit and model selection with a single observed network. *Scientific Reports*, 9(1):16674, 2019.
- Kai-Yang Chiang, Cho-Jui Hsieh, Nagarajan Natarajan, Inderjit S Dhillon, and Ambuj Tewari. Prediction and clustering in signed networks: a local to global perspective. *Journal of Machine Learning Research*, 15(1):1177–1213, 2014.
- James A Davis. Clustering and structural balance in graphs. *Human Relations*, 20(2): 181–187, 1967.
- Tyler Derr, Charu Aggarwal, and Jiliang Tang. Signed network modeling based on structural balance theory. In *Proceedings of the 27th ACM International Conference on Information and Knowledge Management*, pages 557–566, 2018.
- FY Edgeworth. Xlii. the law of error. *The London, Edinburgh, and Dublin Philosophical Magazine and Journal of Science*, 16(100):300–309, 1883.
- Giuseppe Facchetti, Giovanni Iacono, and Claudio Altafini. Computing global structural balance in large-scale signed social networks. *Proceedings of the National Academy of Sciences*, 108(52):20953–20958, 2011.

- Derek Feng, Randolph Altmeyer, Derek Stafford, Nicholas A Christakis, and Harrison H Zhou. Testing for balance in social networks. *Journal of the American Statistical Association*, 117(537):156–174, 2022.
- James H Fowler. Legislative cosponsorship networks in the us house and senate. *Social Networks*, 28(4):454–465, 2006.
- Douglas M Gibling. *International military alliances, 1648-2008*. CQ Press, 2008.
- Alden Green and Cosma Rohilla Shalizi. Bootstrapping exchangeable random graphs. *Electronic Journal of Statistics*, 16(1):1058–1095, 2022.
- Casey S Greene, Arjun Krishnan, Aaron K Wong, Emanuela Ricciotti, Rene A Zelaya, Daniel S Himmelstein, Ran Zhang, Boris M Hartmann, Elena Zaslavsky, Stuart C Sealfon, et al. Understanding multicellular function and disease with human tissue-specific networks. *Nature Genetics*, 47(6):569–576, 2015.
- Peter Hall. *The bootstrap and Edgeworth expansion*. Springer Science & Business Media, 2013.
- Frank Harary. On the notion of balance of a signed graph. *Michigan Mathematical Journal*, 2(2):143–146, 1953.
- Fritz Heider. Attitudes and cognitive organization. *The Journal of Psychology*, 21(1):107–112, 1946.
- Roelof Helmers. On the edgeworth expansion and the bootstrap approximation for a studentized u-statistic. *The Annals of Statistics*, pages 470–484, 1991.
- Wassily Hoeffding. A class of statistics with asymptotically normal distribution. *Breakthroughs in Statistics: Foundations and Basic Theory*, pages 308–334, 1992.
- Peter D Hoff, Adrian E Raftery, and Mark S Handcock. Latent space approaches to social network analysis. *Journal of the American Statistical Association*, 97(460):1090–1098, 2002.
- Douglas N Hoover. Relations on probability spaces and arrays of random variables. *Institute for Advanced Study*, 1979.
- Cho-Jui Hsieh, Kai-Yang Chiang, and Inderjit S Dhillon. Low rank modeling of signed networks. In *Proceedings of the 18th ACM SIGKDD International Conference on Knowledge Discovery and Data Mining*, pages 507–515, 2012.

- Edward L Huttlin, Lily Ting, Raphael J Bruckner, Fana Gebreab, Melanie P Gygi, John Szpyt, Stanley Tam, Gabriela Zarraga, Greg Colby, Kurt Baltier, et al. The bioplex network: a systematic exploration of the human interactome. *Cell*, 162(2):425–440, 2015.
- Edward L Huttlin, Raphael J Bruckner, Jose Navarrete-Perea, Joe R Cannon, Kurt Baltier, Fana Gebreab, Melanie P Gygi, Alexandra Thornock, Gabriela Zarraga, Stanley Tam, et al. Dual proteome-scale networks reveal cell-specific remodeling of the human interactome. *Cell*, 184(11):3022–3040, 2021.
- Jiashun Jin, Zheng Tracy Ke, and Shengming Luo. Mixed membership estimation for social networks. *Journal of Econometrics*, 239(2):105369, 2024a.
- Jiashun Jin, Zheng Tracy Ke, Shengming Luo, and Yucong Ma. Optimal network pairwise comparison. *Journal of the American Statistical Association*, 0(ja):1–25, 2024b. doi: 10.1080/01621459.2024.2393471.
- Alec Kirkley, George T Cantwell, and Mark EJ Newman. Balance in signed networks. *Physical Review E*, 99(1):012320, 2019.
- Jing Lei. Network representation using graph root distributions. *The Annals of Statistics*, 49(2):745–768, April 2021. ISSN 0090-5364,2168-8966. doi: 10.1214/20-aos1976.
- Jure Leskovec, Daniel Huttenlocher, and Jon Kleinberg. Signed networks in social media. In *Proceedings of the SIGCHI Conference on Human Factors in Computing Systems*, pages 1361–1370, 2010.
- Keith Levin and Elizaveta Levina. Bootstrapping networks with latent space structure. *arXiv preprint arXiv:1907.10821*, 2019.
- Robert Lunde and Purnamrita Sarkar. Subsampling sparse graphons under minimal assumptions. *Biometrika*, 110(1):15–32, 06 2022. ISSN 1464-3510. doi: 10.1093/biomet/asac032. URL <https://doi.org/10.1093/biomet/asac032>.
- Robin M Meyers, Jordan G Bryan, James M McFarland, Barbara A Weir, Ann E Sizemore, Han Xu, Neekesh V Dharia, Phillip G Montgomery, Glenn S Cowley, Sasha Pantel, et al. Computational correction of copy number effect improves specificity of CRISPR–Cas9 essentiality screens in cancer cells. *Nature Genetics*, 49(12):1779–1784, 2017.
- Christine Leigh Myers Nickel. *Random dot product graphs a model for social networks*. PhD thesis, Johns Hopkins University, 2008.

- Krzysztof Nowicki and Tom A B Snijders. Estimation and prediction for stochastic block-structures. *Journal of the American Statistical Association*, 96(455):1077–1087, 2001.
- Peter Orbanz and Daniel M Roy. Bayesian models of graphs, arrays and other exchangeable random structures. *IEEE Transactions on Pattern Analysis and Machine Intelligence*, 37(2):437–461, 2014.
- Glenn Palmer, Roseanne W McManus, Vito D’Orazio, Michael R Kenwick, Mikaela Karstens, Chase Bloch, Nick Dietrich, Kayla Kahn, Kellan Ritter, and Michael J Soules. The MID5 Dataset, 2011–2014: Procedures, coding rules, and description. *Conflict Management and Peace Science*, 39(4):470–482, 2022.
- Hein Putter and Willem R van Zwet. Empirical edgeworth expansions for symmetric statistics. *The Annals of Statistics*, 26(4):1540–1569, 1998.
- Hugo Saiz, Jesús Gómez-Gardeñes, Paloma Nuche, Andrea Girón, Yolanda Pueyo, and Concepción L Alados. Evidence of structural balance in spatial ecological networks. *Ecography*, 40(6):733–741, 2017.
- Meijia Shao, Dong Xia, Yuan Zhang, Qiong Wu, and Shuo Chen. Higher-order accurate two-sample network inference and network hashing. *arXiv preprint arXiv:2208.07573*, 2022.
- Weijing Tang and Ji Zhu. Population-level balance in signed networks. *Journal of the American Statistical Association*, 0(ja):1–22, 2024. doi: 10.1080/01621459.2024.2356894. URL <https://doi.org/10.1080/01621459.2024.2356894>.
- Mary E Thompson, Lilia L Ramirez Ramirez, Vyacheslav Lyubchich, and Yulia R Gel. Using the bootstrap for statistical inference on random graphs. *Canadian Journal of Statistics*, 44(1):3–24, 2016.
- David L Wallace. Asymptotic approximations to distributions. *The Annals of Mathematical Statistics*, 29(3):635–654, 1958.
- Bo Wang, Armin Pourshafeie, Marinka Zitnik, Junjie Zhu, Carlos D Bustamante, Serafim Batzoglou, and Jure Leskovec. Network enhancement as a general method to denoise weighted biological networks. *Nature Communications*, 9(1):3108, 2018.
- Larry Wasserman. *All of Nonparametric Statistics*. Springer Science & Business Media, 2006.
- Mingrui Xia, Jinhui Wang, and Yong He. Brainnet viewer: a network visualization tool for human brain connectomics. *PLoS One*, 8(7):e68910, 2013.

- Andrew Zalesky, Luca Cocchi, Alex Fornito, Micah M Murray, and ED Bullmore. Connectivity differences in brain networks. *Neuroimage*, 60(2):1055–1062, 2012.
- Haoran Zhang and Junhui Wang. Signed network embedding with application to simultaneous detection of communities and anomalies. *arXiv preprint arXiv:2207.09324*, 2022.
- Yuan Zhang and Dong Xia. Edgeworth expansions for network moments. *The Annals of Statistics*, 50(2):726–753, 2022.
- Yuan Zhang, Elizaveta Levina, and Ji Zhu. Detecting overlapping communities in networks using spectral methods. *SIAM Journal on Mathematics of Data Science*, 2(2):265–283, 2020.